Thermally Induced Phase Separation in Liquid Crystalline Polymer/Polycarbonate Blends

Kam-Wa D. Lee,[1] Philip K. Chan,[2] Musa R. Kamal[1]

[1]*Department of Chemical Engineering, McGill University, Montreal, Quebec, Canada H3A 2B2*
[2]*Department of Chemical Engineering, Ryerson University, Toronto, Ontario, Canada M5B 2K3*

Received 22 September 2008; accepted 3 June 2009
DOI 10.1002/app.30880
Published online 27 April 2010 in Wiley InterScience (www.interscience.wiley.com).

ABSTRACT: Thermally induced phase separation in liquid crystalline polymer (LCP)/polycarbonate (PC) blends was investigated in this study. The LCP used is a main-chain type copolyester comprised of *p*-hydroxybenoic acid and 6-hydroxy-2-naphthoic acid. Specimens for microscopic observation were prepared by melt blending. The specimens were heated to a preselected temperature, at which they were held for isothermal phase separation. The preselected temperatures used in this study were 265, 290, and 300°C. The LCP contents used were 10, 20, and 50 wt %. These parameters corresponded to different positions on the phase diagram of the blends. The development of the phase-separated morphology in the blends was monitored in real time and space. It was observed that an initial rapid phase separation was followed by the coarsening of the dispersed domains. The blends developed into various types of phase-separated morphology, depending on the concentration and temperature at which phase separation occurred. The following coarsening mechanisms of the phase-separated domains were observed in the late stages of the phase separation in these blends: (i) diffusion and coalescence of the LCP-rich droplets; (ii) vanishing of the PC-rich domains following the evaporation-condensation mechanism; and (iii) breakage and shrinkage of the LCP-rich domains. © 2010 Wiley Periodicals, Inc. J Appl Polym Sci 117: 2651–2668, 2010

Key words: blends; liquid crystalline polymers (LCP); microstructure; polycarbonate; phase separation

INTRODUCTION

Thermally induced phase separation is an important process to manufacture high-performance polymeric materials from various systems, such as polymer solutions,[1,2] polymer blends,[3,4] and biopolymers.[5–7] These practical applications have motivated many studies of the phase separation process, to achieve better understanding and control of the formation of the phase-separated structures in these systems. It has been frequently shown that understanding the phase-separation process is an important step for designing/tailoring the desired structure in these materials. Therefore, extensive studies have been reported on the phase separation in conventional flexible polymer systems (polymer solutions and blends), including both kinetics and mechanisms.[8,9] Solvent casting has been a dominant method for preparing samples, as thin films, to study the thermally induced phase separation behavior. In this method, components are dissolved and mixed well in the same solvent(s). Subsequently, the blends can be used after the solvent is evaporated. Unfortunately, this method is not feasible for polymers that exhibit low solubility to most solvents, in particular, for thermotropic liquid crystalline polymers (LCPs) that are highly resistant to solvents.

Thermotropic LCPs have become an important class of materials in many polymeric applications, especially for producing small-size molded parts.[10] Two commercially available main-chain thermotropic LCPs have been commonly used and studied extensively. They are the copolyesters of *p*-hydroxybenoic acid (HBA) and poly(ethylene terephthalate) (PET),[11–14] and the copolyesters of HBA and 6-hydroxy-2-naphthoic acid (HNA).[15–19] Blending of these LCPs with conventional flexible polymers has also been one of the popular methods for enhancing the mechanical properties of the flexible polymers. These polymer blends commonly separate into two phases: one LCP-rich phase and the other phase is rich in the flexible polymer. In many cases, the phase-separated morphology has a significant impact on the final properties of the blend. The majority of investigations on these blends have been concentrated on the effect of processing conditions on phase miscibility and improvement of mechanical properties.[11,16,20–23] Only a few reports are available on the study of the evolution of the phase-separated

Correspondence to: M. R. Kamal (musa.kamal@mcgill.ca).
Contract grant sponsors: Natural Sciences and Engineering Research Council of Canada (NSERC), CREPEC, McGill University, Ryerson University.

structure in the blends. Kyu and Zhuang[13] prepared HBA-PET type LCP/polycarbonate (PC) blends using a solvent casting method, and studied phase separation behavior employing polarized light microscopy. They observed the development of a highly interconnected structure, as the blends were annealed at 260°C for 10 minutes. Similarly, Nagaya, Orihar, and Ishibashi[14] prepared HBA-PET type LCP/PET blends using the solvent casting method. They showed that the LCP-rich phase appeared mainly as dispersed domains in the phase-separated blends. Moreover, they observed that the thickness of the sample influenced the phase separation process. Thick samples exhibited an increase in the speed of phase separation, and the average size of the dispersed LCP domains became larger. Cohen-Addad et al.[24] examined phase separation in blends of LCP (aromatic, para-linked random copolyester with three monomers) and polysulphone. Their microscopic observations showed that the solvent-cast films exhibited an interconnected structure with large domains ranging from ~ 10 to 30 μm. Moreover, they observed that the rate of phase separation in these blends was much faster than that of solvent evaporation. They indicated that the phase-separated states were thermodynamically stable between 25 and 300°C. Zheng and Kyu[25] also explored morphological development in solvent-cast films of HBA-PET type LCP/polyether sulfone blends. The 50/50 wt % blends developed into interconnected network structure upon annealing at both 250 and 270°C. The speed and extent of phase separation in the blends increased as the annealing temperature was raised. Nakai et al.[26] studied the phase separation and coarsening processes in HBA-PET type LCP/PET blends prepared by the solvent casting method. They used polarized light microscopy to trace the development of the processes. The 50/50 wt % blends underwent thermally induced phase separation in three stages. The LCP-rich phase first developed as a percolating network, and then the LCP-rich network broke up into dispersed droplets. In the final stages, the LCP-rich droplets diffused and coalesced as larger domains. They described the phase separation as spinodal decomposition. However, only the late stages of spinodal decomposition were observed, for a very short annealing time (in a few tens of seconds). In summary, the above studies suggested that the phase-separated structures in blends of LCP and a flexible polymer generally involved interconnected structure and the phase separation process was attributed to spinodal decomposition.

It can be seen that HBA-PET type LCPs have been the common choice for studying the phase separation behavior in their blends with conventional flexible polymers. However, to our knowledge, phase separation in blends involving HBA-HNA type LCPs has not been given similar attention. This is probably because HBA-PET type LCPs can be blended with conventional flexible polymers using the solvent casting method, whereas HBA-HNA type LCPs are insoluble in most organic solvents. In this article, we study the phase separation process in blends of HBA-HNA type LCPs and PC. In a previous work,[27] we constructed the phase diagram of HBA-HNA type LCP/PC blends and showed that the blends undergo phase separation upon heating. The phase diagram of these partially miscible blends consisted of three regions (see Fig. 1 below). Region I denotes conditions that no phase separation was observed. Region II represents phase separation in the blends, which can occur only to a small extent, due to the enhanced molecular chain mobility of the PC phase, while the LCP is still in the nonmolten mesophase. Region III occurs under conditions where PC is in a highly molten state and LCP is in the molten mesophase. Thus, phase separation in the blends can proceed to a larger extent. The present work focuses on the temporal morphological development in these blends, for different positions of the phase diagram. Since solvent casting was not feasible for preparing these blends, the samples were prepared by melt blending. Phase separation in the melt-blended samples was monitored directly, in real time and space, using polarized light microscopy in conjunction with a heating stage.

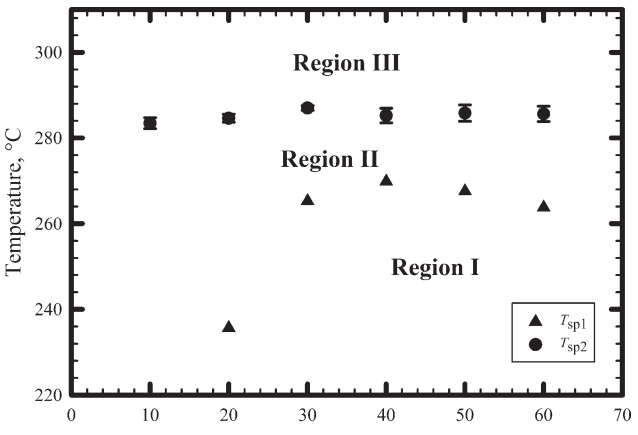

Figure 1 Phase diagram of LCP/PC blends.

EXPERIMENTAL

The HBA-HNA type LCP used in this study was Vectra A950 (Ticona). This random copolyester consists of 73 mol % of HBA and 27 mol % HNA. It has a density of 1.4 g/cm^3, a crystallization temperature of ~ 240°C and a melting temperature of ~ 280°C. The conventional flexible polymer was a commercially available PC (Lexan 121, G.E. Plastics). This

PC has a density of 1.2 g/cm^3, a glass transition temperature of $\sim$ 145°C and melt flow index of 17 g/10 minutes. These components were blended in a twin screw extruder attached to a circular die. Specimens for microscopic observation were sectioned from the core region of the extrudate, using an Ultracut microtome. Details of these processing methods are described in our previous work[27] and are not repeated in this article. Hence we describe below only the additional methods employed in this study.

The temporal morphological development of the blends was observed with a polarized light microscope (PLM) (Olympus BX50) equipped with a shear stage (Linkam CSS450). The shear stage was solely used as a heating device and for controlling the thickness uniformity of the microscopic specimens throughout the experiments. Early results indicated that the sample thickness influenced the speed of phase separation.[14] Therefore, it was necessary to ensure uniform thickness of the sample, to obtain a uniform speed of phase separation across the sample. A 530 nm compensator was inserted between the polarizer and analyzer, in all the experiments, for the purpose of obtaining good contrast of the phase-separated structure in the samples. With the above arrangement, the transparent PC-rich phase appeared as violet (due to the background color) and the LCP-rich phase emerged as brownish-yellow. This observation has also been confirmed with fourier transform infrared (FTIR) microscopy presented in Appendix A.

Experiments were started by heating the specimens from room temperature to 200°C at 30°C/min (maximum available rate for the shear stage). After holding at 200°C for 15 minutes, specimens were further heated at 30°C/min to the designated temperature for phase separation. The phase separation temperatures used in this work were 265, 290, and 300°C. The concentrations used were 10, 20, and 50 wt % LCP. The gap size of the sample cell was controlled at 30 μm for all the experiments. Real time images of the specimens were captured with a video camera (Sony Power HAD 3CCD Color) every 4 seconds.

RESULTS AND DISCUSSIONS

It is known that transesterification (TE) between LCPs and PCs may occur during the blending process. Thus, such a possibility should be taken into consideration, since such a chemical reaction would generate block copolymers at the interface between the two components, and consequently alter the phase behavior of the blends. We investigated this possibility in our earlier work, using nuclear magnetic resonance (NMR) spectroscopy and FTIR spectroscopy. These results were presented and discussed elsewhere.[27] So, they are not discussed here. In summary, TE did not seem to occur to a significant extent during the blending process, due to a number of factors, including the thorough drying of the components before blending, the low extrusion temperature (270°C at the die) and the short residence times during blending.

Figure 1 shows the phase diagram of HBA-HNA type LCP/PC blends, constructed and reported in our previous work.[27] This phase diagram can be considered as a lower critical solution temperature type, because phase separation occurs in the blends with increasing temperatures. It is divided into three regions with two phase separation temperatures, T_{sp1} and T_{sp2}, as internal boundaries. Only small morphological changes are observed between T_g of PC (145°C) and 200°C, i.e., when the temperature is below T_{sp1} (Region I). Blends in this region are mainly in the solid state. Therefore, the morphology in this phase will not be discussed. On the other hand, significant phase separation is observed, when the temperature is between T_{sp1} and T_{sp2} (Region II), and more pronounced phase separation occurs, when the temperature is above T_{sp2} (Region III). Blends in Region II consist of a PC phase in the molten state and LCP phase in nonmolten mesophase state. This is because temperatures in this region are significantly above the T_g of PC, but below the T_m (melting peak temperature) of LCP. Therefore, Region II is a coexistence region consisting of isotropic liquid and nonmolten nematic. Region III is the area where the temperatures are above T_m of LCP. This means that both PC and nematic LCP are in the molten state. Therefore, this region can be considered as an isotropic liquid + molten nematic coexistence region. It should be noted that nematic to isotropic transition of LCP was not determined. This is because the corresponding temperature is usually higher than the commonly used processing temperatures, and probably higher than the degradation temperature. The present work deals mainly with morphological changes in the Regions II and III.

Phase separation in Region II

Figure 2 shows the microscopic images of the changes in morphological structure for 10 wt % (first row), 20 wt % (second row) and 50 wt % (third row) LCP/PC blends at a phase separation temperature of 265°C. This temperature is located in Region II of the phase diagram. Images in the first, second and third columns represent structures after holding at 200°C for 15 minutes, structures upon reaching 265°C and structures at 265°C after 60 minutes for these blends, respectively. The 10 wt % LCP/PC

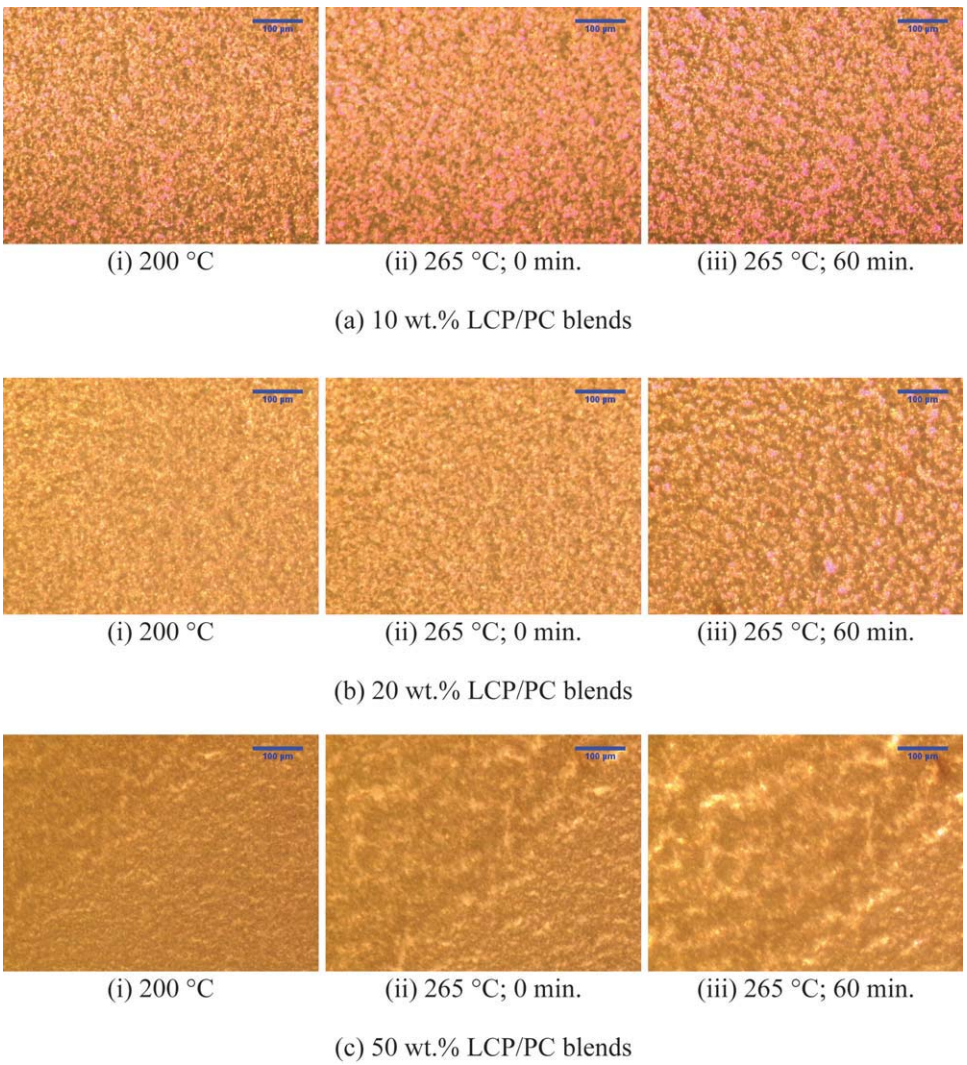

Figure 2 Phase separation in LCP/PC blends at 265°C. Scale bar on images represents 100 μm. [Color figure can be viewed in the online issue, which is available at www.interscience.wiley.com.]

blends exhibit coarse-grained texture at 200°C. Both the PC-rich phase (pink color) and the LCP-rich phase (yellow-brown color) are observed at this temperature. This indicates that this blend has already undergone a certain extent of phase separation and can exhibit a stable phase-separated structure at a temperature as low as 200°C. The extent of phase separation becomes more significant, as the temperature is raised to 265°C, as indicated by the more pronounced pink color of the PC-rich domains. After the phase separation is allowed to occur for 60 minutes at 265°C, larger and more distinguishable PC-rich domains (pink) emerge. In this co-continuous phase-separated structure, the LCP-rich phase appears predominantly as the minor phase with irregular shapes, whereas the PC-rich phase is clearly the major phase. Blends with 20 wt % LCP exhibit a fine-grained texture at 200°C and do not show significant changes upon heating to 265°C. However, after annealing for 60 minutes at 265°C, more PC-rich domains become visible and the blend develops into a more pronounced phase-separated structure. In contrast to the 10 wt % LCP/PC blends, the separated phases in this blend are less distinguishable. The 50 wt % LCP/PC blends exhibit only small changes in morphology, with slightly phase-separated structure appearing after the blends are annealed at 265°C for 60 minutes. The PC-rich phase can be barely seen in a few regions on the image [very pale pink areas in Fig. 2(c)-iii]. It should be noted that these areas had a violet color and were clearly identified under microscopic observation. The small changes in structure suggest that the 50 wt % blends have relatively limited susceptibility to phase separation, under the conditions considered. This can be explained by the lower mobility of the 50 wt % blends, because they contain less PC (compared to the 10 and 20 wt % LCP/PC blends).

The above microscopic observations indicate that the extent of phase separation in LCP/PC blends

occurring at 265°C (i.e. Region II in the phase diagram) depends strongly on the composition of the blends. Blends with high content of PC exhibit a large degree of phase separation, whereas blends with low PC content undergo limited phase separation. This is because the overall chain mobility in the blends is concentration dependent. These observations imply that molecular mobility of PC controls the phase separation process at 265°C, which is ~ 120°C above the glass transition temperature of PC. However, it is ~ 15°C below the melting temperature of LCP. At this temperature, PC segments exhibit high mobility, whereas the LCP segments have limited molecular mobility. In other words, the molecular chain mobility of PC is significantly larger than that of LCP at this temperature. As a result, the overall mobility in the blends, which is important for phase separation, is mainly due to the contribution of the PC phase, and the extent of phase separation depends strongly on the PC content. The overall mobility in the blends can be related to the individual mobility of the component from either the slow or fast mode theory.[28] The slow mode theory predicts that the slow diffusing component dominates the overall mobility, while the fast mode theory suggests that the fast diffusing component controls the overall mobility. Both theories produce essentially the same phase-separated structure. However, they differ in the time scale for achieving the same extent of phase separation.[29] In the current case (phase separation at 265°C), PC is considered as the fast component and LCP is the slow component. Consequently, it can be deduced that phase separation of LCP/PC blends occurring at 265°C follows the fast mode theory, and it is controlled by the PC phase.

Phase separation in Region III—Shallow regime

Figure 3 shows the microscopic images of morphological development in 10 wt % (first row), 20 wt % (second row) and 50 wt % (third row) LCP/PC blends undergoing phase separation at 290°C, which is located in the shallow regime of Region III of the phase diagram. This means that it is slightly above the internal boundary that divides Region II and Region III on the phase diagram. Moreover, this temperature is ~ 10°C above the peak melting temperatures of the above blends, which is the melting temperature of the LCP phase.[27] Therefore, phase separation occurs in the true melt state. The images in the first, second and third columns, represent the structures of these blends after holding at 200°C for 15 minutes, upon reaching 290°C and after holding for 20 minutes at 290°C, respectively. As in the case of 265°C, the 10 wt % LCP/PC blends emerge as a slightly phase-separated structure at 200°C and appear as a coarse-grained texture. Blends with 20 and 50 wt % LCP, on the other hand, do not show obvious phase-separated structure and appear as a fine-grained texture. As the blends are heated to 290°C, for all the concentrations used in this case, well defined phase-separated structures can be identified. This indicates that the phase segregation power is much stronger in this case than that in the case of 265°C. The phase segregation power refers to the thermodynamic driving force to maintain the phase separation process. For the LCP/PC blends, the phase segregation power is enhanced as temperature increases.[26] In fact, phase separation starts before reaching 290°C. Upon further annealing isothermally at 290°C, the phase-separated domains grow and increase very rapidly within 1–2 minutes. No further growth of the phase-separated domains is observed, even if the isothermal annealing is allowed to continue for longer time. The phase-separated structures with various LCP contents after annealing for 20 minutes are shown in the third column of Figure 3.

The stronger phase segregation power at 290°C than that at 265°C can be attributed to the higher driving force at the elevated phase separation temperature. The increased driving force promotes the speed and extent of phase separation in the blend. Moreover, the stronger phase segregation power can also be related to the increased overall mobility of the blends. By raising the phase separation temperature from Region II in the phase diagram to Region III, LCP segments gain substantial mobility. Recall that the overall mobility to achieve phase separation in the blends depends on the individual molecular chain mobilities of the two components. Higher overall mobility in the blends yields a faster phase separation process. Therefore, the substantial rise in the mobility of the LCP segments at the higher phase separation temperature raises the overall mobility in the blends. Consequently, it promotes the speed and extent of phase separation.

Phase separation in polymer blends can produce various phase-separated structures, depending on the concentrations of the components. In the present study, the 20 wt % LCP/PC blends produced an interconnected structure. This structure is one of the characteristics of spinodal decomposition for systems with concentration near the critical regions of the phase diagram, which has frequently been reported from both experimental and numerical studies for binary polymer systems undergoing spinodal decomposition.[30–34] Analysis of spinodal decomposition in this blend, using fast fourier transform (FFT) digital image analysis of the original optical microscopy images, is shown in Appendix B. This analysis supports the conclusion that phase separation in these blends occurs by spinodal decomposition.

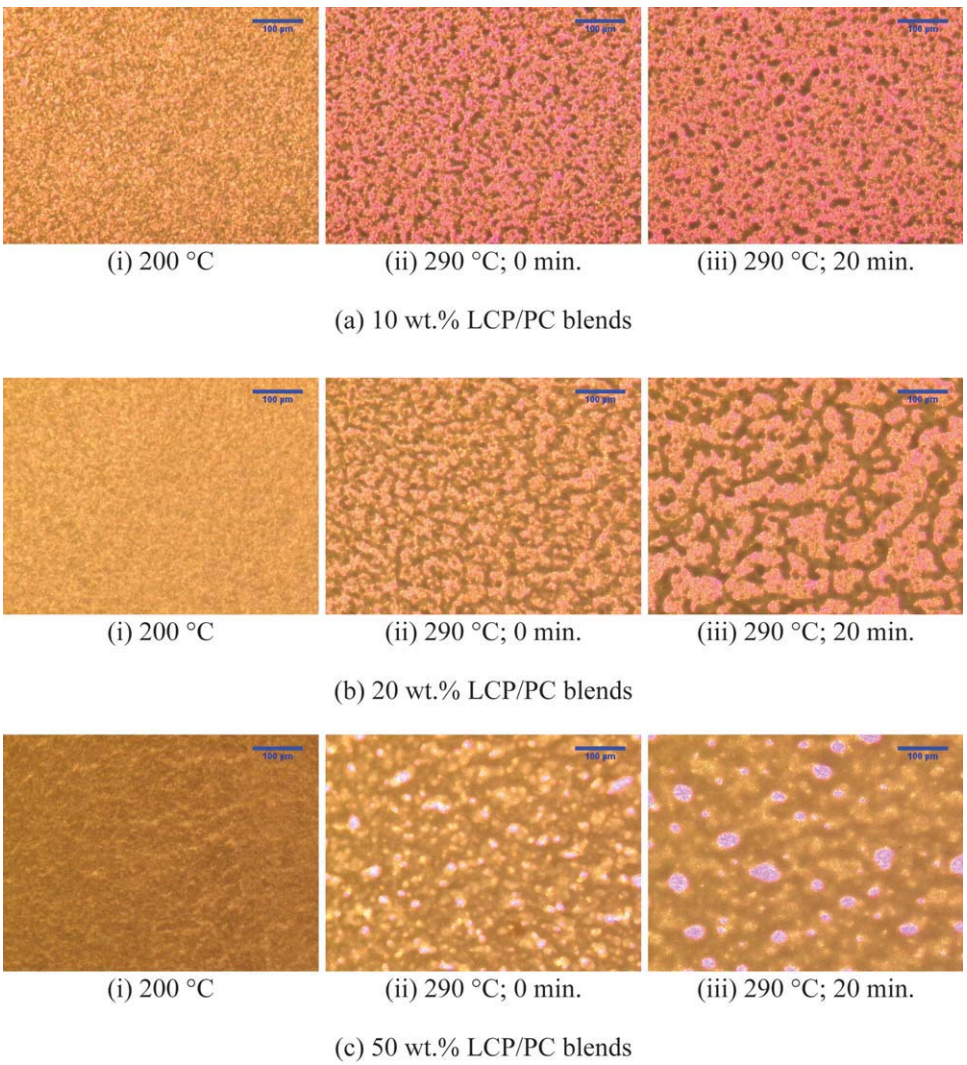

Figure 3 Phase separation in LCP/PC blends at 290°C. Scale bar on images represents 100 μm. [Color figure can be viewed in the online issue, which is available at www.interscience.wiley.com.]

Blends with 10 and 50 wt % of LCP developed different structures. For the 10 wt % LCP/PC blends, the LCP-rich phase appeared as isolated domains, dispersed in the PC-rich phase. This is because the LCP is the minor component in this case. For the 50 wt % LCP/PC blends, the PC-rich phase formed near-circular domains and dispersed in the LCP-rich phase. These two structures (droplet-type) indicate that the 10 and 50 wt % LCP blends are located in the off-critical (i.e., away from the critical concentration) regions in the phase diagram. This type of structure has also been recognized, from experimental and numerical works, in binary polymer systems undergoing spinodal decomposition.[30–34]

Phase separation in Region III—Deep regime

To investigate the phase separation via spinodal decomposition in the LCP/PC blends, the phase separation temperature was further raised to 300°C. This temperature is located in the deep regime of Region III of the phase diagram. Phase separation at this temperature should occur to a larger extent than in the above two cases. Figure 4 shows the micrographs of the morphological development of (a) 10 wt % LCP/PC blends, (b) 20 wt % LCP/PC blends and (c) 50 wt % LCP/PC blends at various temperatures, upon reaching 300°C for isothermal annealing. In general, no clear phase-separated structures could be observed, when the temperature is below ~ 280°C. However, the blends were transformed rapidly (i.e., in 20 seconds) to phase-separated structures, when the temperature reached 290°C. At this temperature, both the LCP-rich phase and the PC-rich phase can be identified clearly. As the temperature was further increased to 300°C (i.e., after another 20 seconds), the phase-separated domains grew rapidly.

As in the case of the above observations at 265 and 290°C, the 10 wt % LCP/PC blends exhibited a

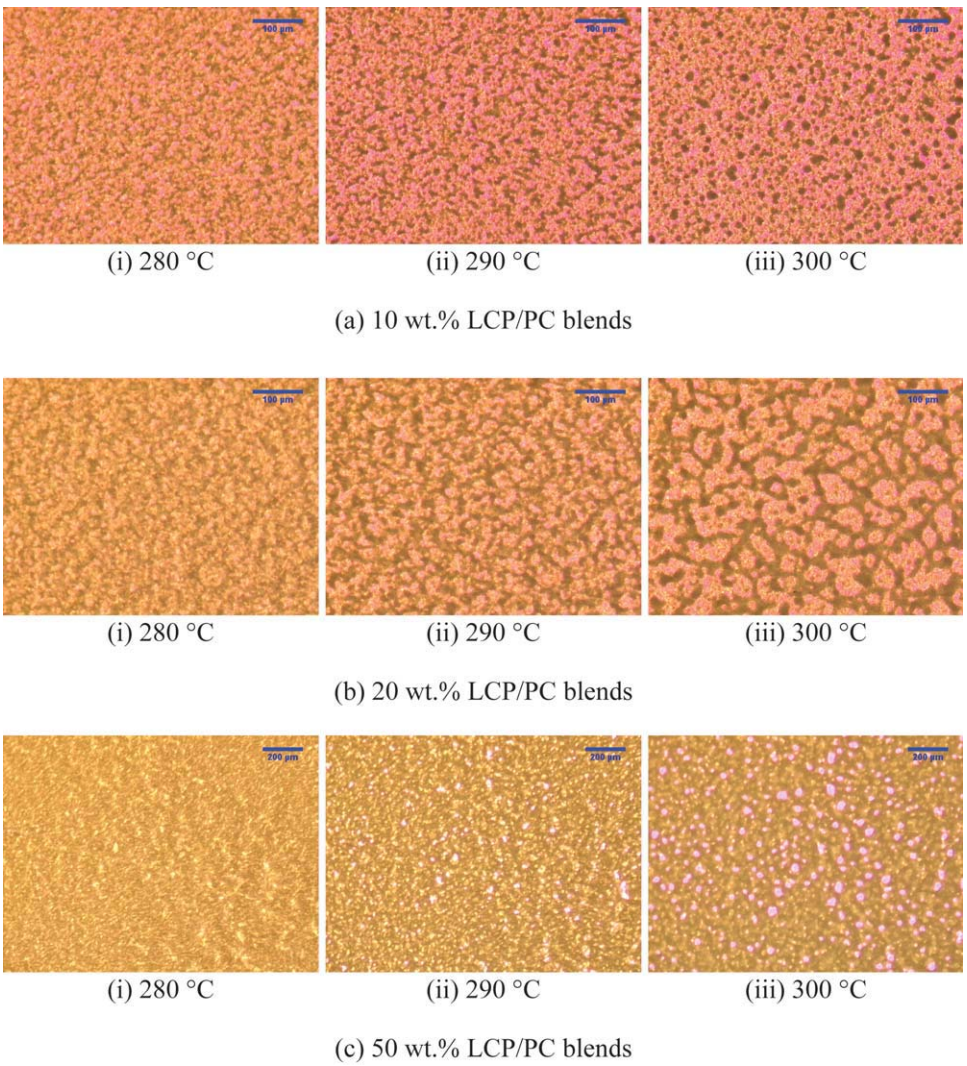

Figure 4 Development of phase-separated structure in LCP/PC blends in the early stage at 300°C. Scale bar on images represents 100 μm. [Color figure can be viewed in the online issue, which is available at www.interscience.wiley.com.]

slightly phase-separated state in the low temperature range (200–270°C), despite the high molecular chain mobility of the PC phase. The PC-rich phase became more visible as the temperature was increased to 280°C. Conversely, the blends quickly changed to a distinguishable phase-separated structure as the temperature reached 290°C. This means that the speed of phase separation increased considerably, because the blend position moved from Region II to Region III on the phase diagram. Thus, the blends became more unstable, which promotes the phase separation. As the temperature reached 300°C, phase separation appeared to continue with near-circular LCP-rich domains dispersed in the PC-rich matrix. Such LCP-rich domains have been observed frequently in various studies relating to HBA-HNA type LCP/PC blends.[35,36]

Blends with 20 and 50 wt % LCP did not show clear phase-separated structures below 280°C. These blends changed from fine-grained texture to coarse-grained texture, as the heating progressed. However, predominantly phase-separated structures could be clearly observed, only when the temperature reached 290°C. At this temperature, as described above, the 20 wt % LCP/PC blends developed an interconnected structure, whereas, the 50 wt % LCP/PC blends evolved into a droplet-type structure. When the temperature reached 300°C, the LCP-rich phase in the 20 wt % LCP/PC blends was progressively transformed from the interconnected network into fragments. Moreover, the fragments collapsed into isolated droplets in several regions [see Fig. 4(b)-iii]. This characteristic morphological development of spinodal decomposition is similar to that reported for other blends of LCP (HBA-PET type) and thermoplastic polymers.[13,14] The behavior of 50 wt % LCP/PC blends was different from that of the 20 wt % LCP/PC blends. The former erupted into droplet-type structure, where the PC-rich phase was dispersed in the LCP-rich phase. When the

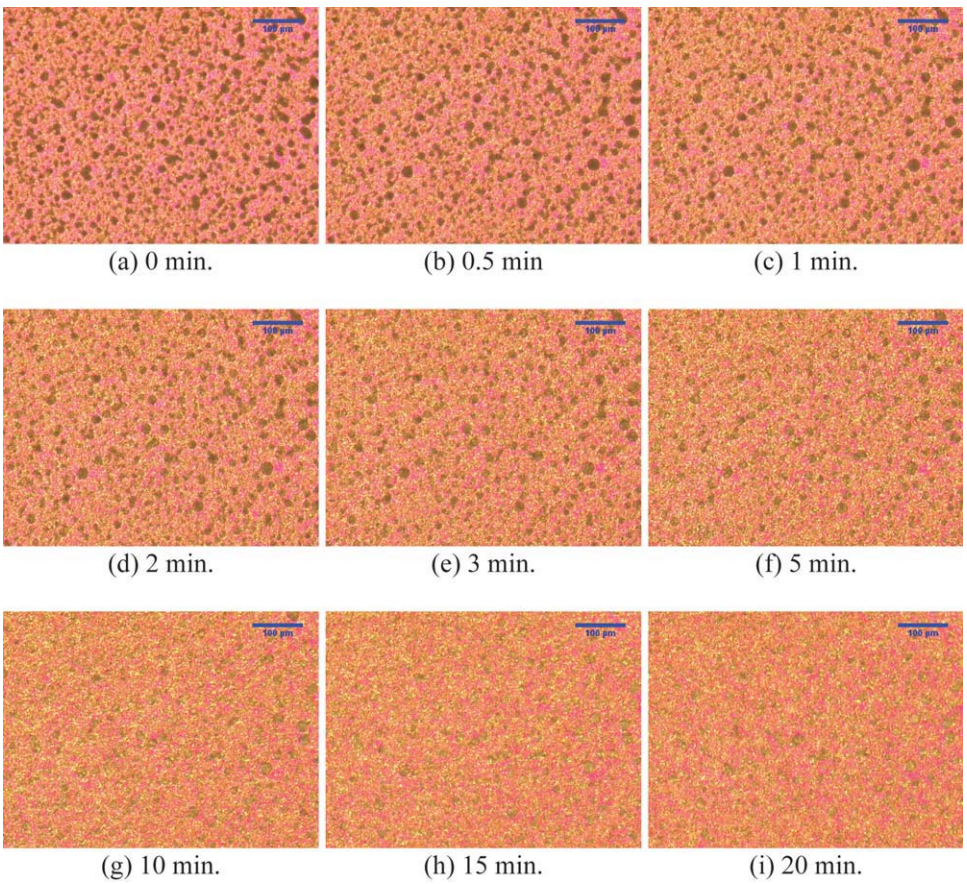

Figure 5 Development of phase-separated morphology in 10 wt % LCP/PC blends in the late stages at 300°C. Scale bar on images represents 100 μm. [Color figure can be viewed in the online issue, which is available at www.interscience.wiley.com.]

temperature reached 300°C, the PC-rich domains increased in size and some coarsening of droplets was observed occasionally. This indicated that the phase separation reached the intermediate to late stages of spinodal decomposition. It should be pointed out that dispersion of the PC phase within the LCP phase has been rarely reported in literature.[36] In summary, phase separation in HBA-HNA type LCP/PC blends occurred rapidly upon entering Region III of the phase diagram. Within a very short period of time (less than 40 seconds), the process reached the intermediate stage of spinodal decomposition.

The phase-separated structures in the blends continued to grow with time upon isothermal annealing at 300°C. This period corresponds to the late stages of spinodal decomposition. Figure 5 shows the time evolution of the phase-separated domains in 10 wt % LCP/PC blends after reaching 300°C. It should be noted that the times indicated for these images stand for the isothermal annealing time at 300°C. These values do not represent the time since phase separation started, because the process started before reaching 300°C. This also applies to the cases describe in Figures 6–8 in below. During the first minute of isothermal annealing, the cross sections of the LCP-rich domains became more circular, to minimize the interfacial area. However, the phase-separated pattern and the size of the dispersed domains in the blend did not show substantial changes with elapsed time, because the phase separation process reached the equilibrium state. It should be pointed out that the sizes of the dispersed LCP-rich domains were not uniform. A broad size distribution, from a few microns to tens of microns, was obtained. The LCP-rich domains appeared as three-dimensional droplets, when they were smaller than the sample thickness (30 μm).

Figure 6 shows the time evolution at 300°C of phase-separated morphologies in 20 wt % LCP/PC blends. In contrast with the behavior of the 10 wt % LCP/PC blends, both the phase-separated pattern and the size of the domains changed with elapsed annealing time. The breakup of the interconnected network into fragments continued. After 1 minute of the isothermal annealing [compare Fig. 6(a,c)], connectivity of the LCP-rich phase was significantly reduced, with the LCP-rich phase appearing as

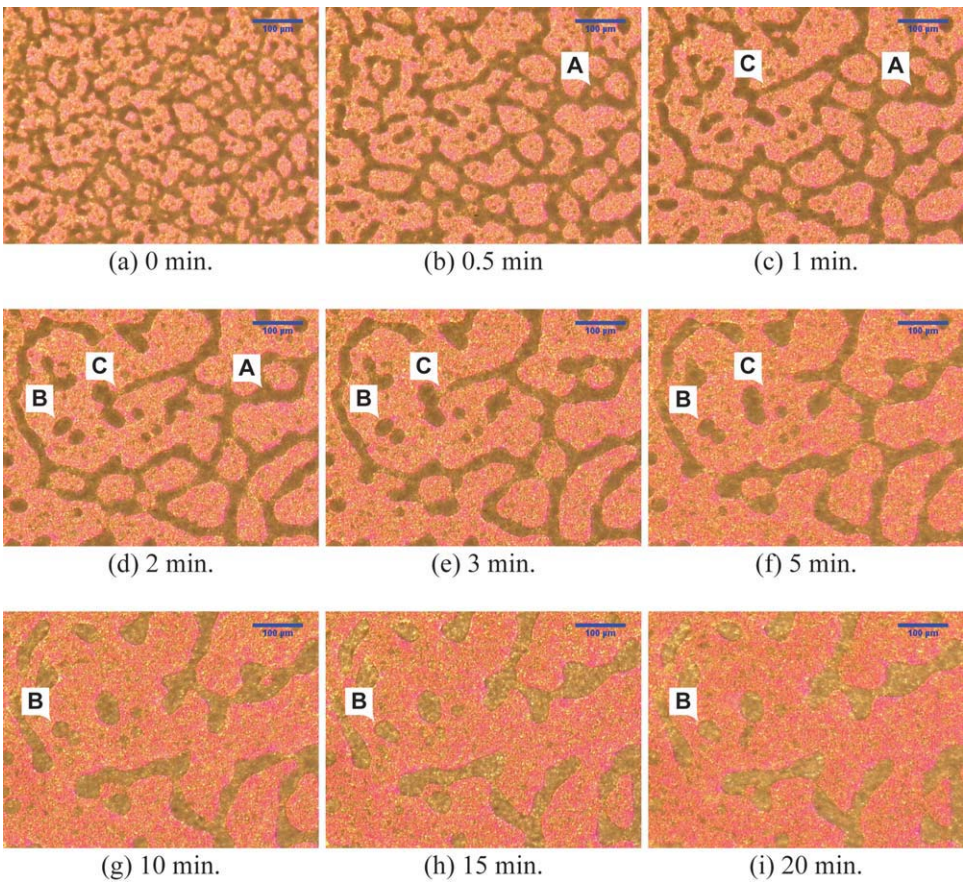

Figure 6 Development of phase-separated morphology in 20 wt % LCP/PC blends in the late stages at 300°C. Scale bar on images represents 100 μm. [Color figure can be viewed in the online issue, which is available at www.interscience.wiley.com.]

fragments. In some regions, the LCP-rich phase appeared as isolated domains with near-circular shape. As phase separation continued, the LCP-rich fragments became shorter in length but wider [see Fig. 6(f)]. At the same time, more isolated LCP-rich domains were formed. Coarsening of smaller droplets into larger droplet was also observed in a few regions in the blends. The changes of the phase-separated morphology in the blends slowed down with further annealing. The sizes of the LCP-rich fragments and the isolated large droplets (i.e., formed from breakup of the interconnected network) appeared to be larger than the sample thickness. Therefore, the domains grew mainly in two-dimensional space. Small LCP-rich domains could also be seen in the PC-rich phase. These small particles were also observed in the early and intermediate stages of spinodal decomposition [see Fig. 4(b)]. This suggested that the small LCP-rich domains did not originate solely from the breakup and shrinkage of the LCP-rich network, but also possibly from the phase separation occurring in the PC-rich phase. Blends with low LCP contents exhibit very strong tendency for phase separation to produce LCP-rich domains, a few microns in diameter. Such small domains can undergo three-dimensional growth. Accordingly, phase-separated domains via spinodal decomposition in these blends result in two different sizes: the large domains (i.e., through the formation and shrinkage of the LCP-rich interconnected network) and the phase separation of smaller LCP rich domains within the phase-separated PC-rich phase.

The temporal development of the phase-separated morphology in the late stages of spinodal decomposition in the 50 wt % LCP/PC blends is shown in Figure 7. The phase-inverted pattern (i.e., PC-rich phase dispersed in the LCP-rich phase) continued to grow. After isothermal annealing for 5 minutes, the morphology was quite uniform and the PC-rich domains took on a near-circular shape with diameter $\sim$ 100 μm. This phase-separated structure remained unchanged (except for the slow growth of the PC-rich domains), after 20 minutes of annealing. This behavior is different from observations reported for blends of LCP (HBA-PET type) and PET (50 wt % LCP) annealed at 270°C.[26] The HBA-PET type LCP-rich phase appears initially as a "percolating network". During the later stages of spinodal decomposition ($\sim$ 7 minutes of annealing time) of this LCP/PET blend, the network was broken-up and shrunk,

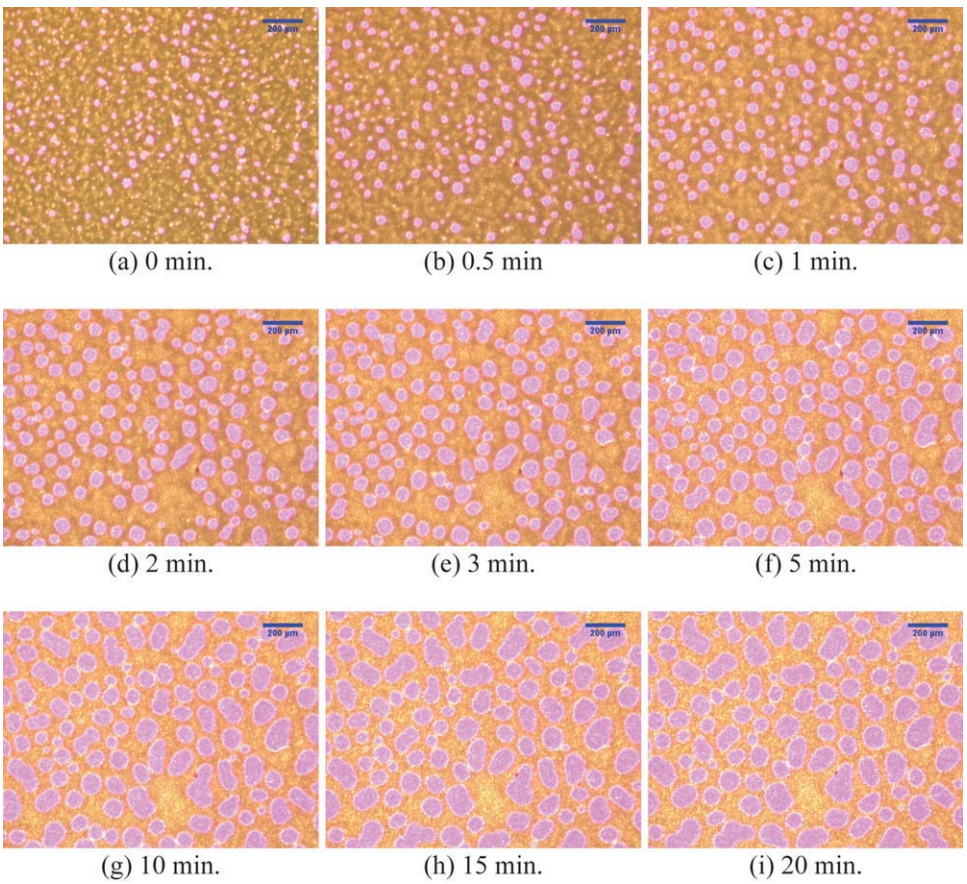

Figure 7 Development of phase-separated morphology in 50 wt % LCP/PC blends in the late stages at 300°C. Scale bar on images represents 200 μm. [Color figure can be viewed in the online issue, which is available at www.interscience.wiley.com.]

and the LCP-rich phase was transformed into isolated circular droplets dispersed in the PET-rich phase. However, in the present work, the phase-inverted morphology remained the same, even though the annealing was allowed to continue for 60 minutes (image not shown). This is probably because the 50 wt % LCP/PC blends in Region III do not correspond to the critical composition on the phase diagram.

Coarsening of the phase-separated domains in the late stages may occur according to several coarsening mechanisms, depending on the contents of the components in the blends. At the microscopic scale, which occurs mainly in blends with low LCP content (e.g. 10 wt % or less), the dispersed domains float in a three-dimensional space and move randomly with Brownian-like motion. Amalgamation into larger domains depends on the frequency of collisions among the isolated domains. This diffusion-coalescence mechanism is a well-known in spinodal decomposition.[37] Co-existence of dispersed domains at the macroscopic scale emerges, when the LCP content in the blends increases. For example, a wide variety of dispersed sizes and shapes can be seen in the phase-separated morphology in the 20 wt % LCP/PC blends. In such a case, three additional phase ordering schemes can take place: (i) vanishing of PC-rich domains; (ii) coagulation of isolated LCP-rich domains; and (iii) breakup of LCP-rich network. It is likely that the above three coarsening mechanisms could occur simultaneously in the same time span.

The vanishing of the PC-rich domains may be considered to follow the evaporation-condensation mechanism.[38] According to this mechanism, molecules in the small PC-rich domains (labeled as A on the images of Fig. 6) diffuse through the LCP-rich domains and merge into the adjacent larger PC-rich domains. Another domain coarsening mechanism present in the 20 wt % LCP/PC blends is the coagulation of isolated LCP-rich droplets (indicated as B on images of Fig. 6). In this illustration, two large near-circular LCP-rich domains come close together. Recall that these two domains were formed from the breakup of the LCP-rich network and they grew in two-dimensional space. The two droplets eventually touch each other and finally amalgamate as one. Similar observations were reported for blends of

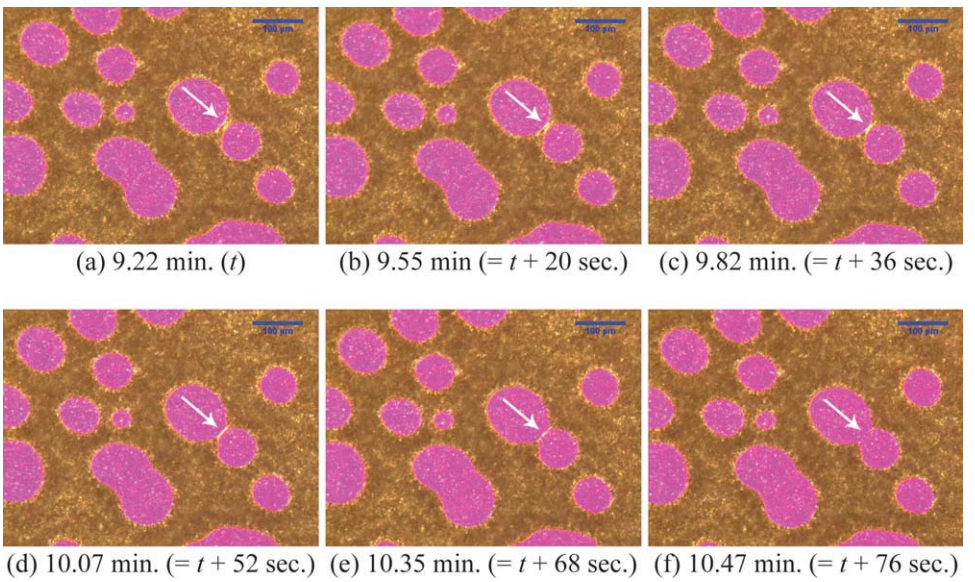

Figure 8 Illustration of coarsening of PC-rich droplets in 50 wt % LCP/PC blends at 300°C at high magnification. Scale bar on images represents 100 μm. [Color figure can be viewed in the online issue, which is available at www.interscience.wiley.com.]

LCP (HBA-PET) and PET.[14] It should be noted that, in the LCP/PET studies, the sample was placed on a piece of microscopic slide, in which one side of the sample was in contact with the glass, while the other side was in contact with air (i.e. a free surface). The interfacial tension between the surface of the sample and the air was different from the interfacial tension between the sample and the glass. It has been suggested that this difference in surface tension initiates the coarsening of the LCP-rich droplets.[14] In fact, no coarsening was observed when the sample was sandwiched between two pieces of microscopic glass.[14] In the present study, coalescence of LCP-rich droplets was seen clearly, even though the sample was placed between two glass slides. Therefore, our observations do not support the hypothesis regarding coalescence of droplets due to the above differences in interfacial tension. It seems that coarsening of droplets in the present study follows the diffusion-coalescence mechanism, but the diffusion rate is much slower than in the case of the microscopic particles.

The third domain coarsening mechanism during the late stages in 20 wt % LCP/PC blends is the breakup and shrinkage of the LCP-rich network-like domains (labeled as C in Fig. 6). In this case, the pressure gradient created by the local curvatures of the LCP-rich interfaces causes the convective motion of the domains. The convective motion leads to the elongation of the domains, to reduce the pressure gradient. The elongated domains exhibit changing diameters along the length of the fragment, which results in variation of capillary pressure in that direction. This variation of capillary pressure drives the breakup of the LCP-rich network-like domains.[39] In general, domains with small diameter have higher capillary pressure than domains with larger diameter. This capillary pressure gradient generates flow of LCP segments from the narrow portion toward the larger portions, and, eventually, the long fragment breaks into shorter fragments and causes coarsening of the LCP-rich domains.

The breakup of the LCP-rich domains was also observed in the 50 wt % LCP/PC blends. In contrast with the 20 wt % LCP/PC blends, this breakup caused the coarsening of the PC droplets. Figure 8 illustrates the coarsening of two PC droplets into one larger droplet at high magnification (from separate experiments). As the dispersed PC droplets continue to grow, the LCP-rich domains (thin layers) that surround and separate the two PC droplets become more elongated and thinner (indicated by the arrows in Fig. 8). The capillary pressure gradient causes flow from the thin part to the bulk region of the LCP-rich phase. The flow exerts local instability and causes breakup of the thin elongated fragment.

In addition to the breakup of the LCP-rich domains, the elongated portion clearly shows different color from the bulk regions. The bulk regions appear as brownish-yellow, while the elongated LCP-rich domains appear as bright yellow. The yellow color becomes brighter as the elongation of the domains becomes more pronounced. It is well known that LCP molecules can be made to align in flow fields and thus exist in the form of elongated fibrils.[40] Therefore, it is suggested that the change of color in the thin elongated LCP-rich domains is probably due to the realignment of the LCP

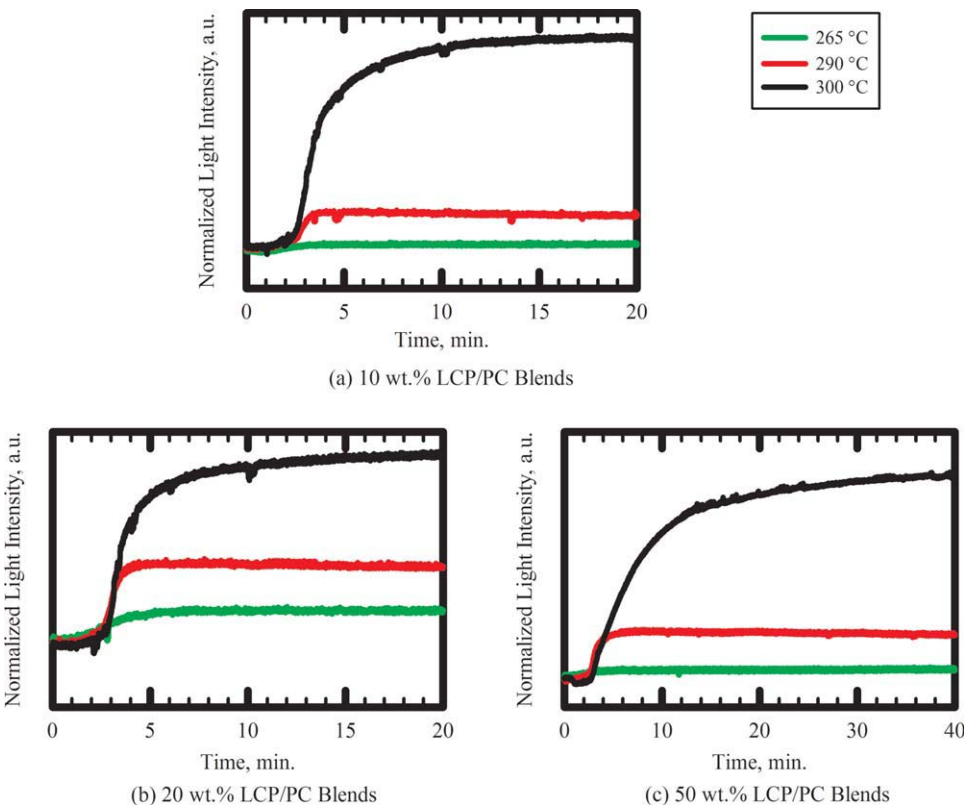

Figure 9 Transmitted light intensity for LCP/PC blends undergoing phase separation at various temperatures. [Color figure can be viewed in the online issue, which is available at www.interscience.wiley.com.]

molecules (i.e., follows the director reorientation of the nematic phase). Thus, the bright yellow color might indicate that the LCP molecules are oriented in the same direction under the polarized light (either parallel or perpendicular to the optical path of the microscope). In the present case, the bright yellow color is more likely to indicate that the LCP molecules are aligned perpendicular to the optical path. However, other factors might also contribute to the observed change of color. Careful examination of the images in Figures 5–7 shows that the appearance of bright yellow as the majority color of the LCP-rich phase usually occurs in the very late stages of the annealing. This implies that reorientation of LCP molecules (nematic ordering) lags behind phase separation (concentration ordering) in the blends. This observation is in agreement with the numerical results of phase separation in blends of LCP and flexible polymers.[41]

Light transmission measurements

Measurement of light transmittance is one of the possible ways to study phase separation induced by temperature in polymer blends containing liquid crystal phases. Ahn et al.[42] investigated the temperature-induced phase separation in a blend of side-chain liquid crystal polymer and a low molecular weight liquid crystal. In their experiments, the transmittance of the sample films as a function of temperature was measured under cross-polarized light. They proposed that the variation of the transmittance of the sample films was the result of microphase separation and transformation of different phases within the sample. Moreover, our previous studies[27] showed that the transmitted light intensity of a sample film during a given experiment correlated well with the extent of phase separation in the HBA-HNA type LCP/PC blends in the range of 280–300°C.

Figure 9 shows the changes of the normalized intensity of transmitted light, I_{tm}, passing through the LCP/PC blends from the light source to the eyepiece of the microscope, during phase separation experiments at various temperatures. The details of the apparatus and the measurement technique have been described elsewhere.[27] Briefly, a flexible optical fiber was connected from the eyepiece to a photomultiplier detector; and the variation of I_{tm} was recorded using a data acquisition system. Earlier studies have indicated that I_{tm} shows a linear correlation with the extent of phase separation that occurs during an individual experiment.[27] In this study, I_{tm} values were recorded from the initial heating step to the end of the experiment.

Figure 9 shows that, for all experiments, I_{tm} remained fairly constant initially. Then, it increased

to reach a plateau with no further obvious changes. Thus, the phase separation in the blends can be divided into three periods. The first period is approximately 2–3 minutes (depending on the final temperature for undergoing phase separation). It includes the heating step and the early stages of spinodal decomposition. During this period, I_{tm} remains consistently low, before phase separation occurs in the blends. When phase separation starts, I_{tm} begins to increase. Moreover, when phase separation experiment is conducted at high temperature, I_{tm} begins to rise before the temperature reaches the designated level. This happens because the driving force for phase separation is strong and causes separation to occur during the heating step.

The second period corresponds to the intermediate to late stages of spinodal decomposition. The phase-separated blends continue to grow through the concentration ordering and the coarsening of the dispersed domains. In this time interval, I_{tm} increases rapidly, indicating that phase separation in the blends is occurring at a high rate. The length of this period varies according to the temperature of isothermal annealing. It is short when the temperature is low (e.g., 265°C); and long when the temperature is high (e.g. 300°C). Moreover, the increment of I_{tm} varies with the isothermal annealing temperatures, because when the annealing temperature changes, the phase separation process takes place at different positions of the phase diagram. Thus, the blends exhibit different overall molecular mobility and driving power for phase separation. Phase separation at 265°C takes place in Region II of the phase diagram, where the blends exhibit low overall molecular mobility and driving power. Therefore, the blends are only slightly phase-separated. On the other hand, phase separation at 300°C takes place in the deep regime of Region III of the phase diagram, where the blends possess high overall molecular mobility and driving power for phase separation. As a result, phase separation in the blends can proceed to a higher extent.

The third period corresponds to the late stages of spinodal decomposition. In this period, the increment of I_{tm} decreases and, eventually, I_{tm} remains constant. The gradual increase of I_{tm} in this stage reflects the fact that the development of the phase-separated morphology in the blend slows down. This is because phase separation in the blends is predominantly controlled by the coarsening of the phase-separated domains. The growth of I_{tm} stops when the phase-separated structure is pinned at the equilibrium state.

CONCLUSIONS

Phase separation in blends of HBA-HNA type LCP and PC was investigated with polarized light microscopy, in conjunction with a hot stage. Melt-blended specimens with 10, 20, and 50 wt % LCP were allowed to undergo phase separation at various temperatures of 265, 290, and 300°C. The results showed that the blends developed different phase-separated morphologies, according to the LCP content. For the 10 wt % LCP/PC blends, the LCP-rich domains appeared as nearly spherical droplets dispersed in the PC-rich matrix. In the 20 wt % LCP/PC blends, the dispersed LCP-rich domains appeared in various sizes and shapes, while in the 50 wt % LCP/PC blends, the dispersed PC-rich phase exhibited a nearly circular cross-section. Furthermore, small LCP-rich domains, a few microns in diameter, co-existed with the above dispersed domains. These small LCP-rich domains were observed in the phase-separated PC-rich domains regardless of the concentration of the blend.

The temperatures for isothermal annealing used in this study corresponded to different positions on the phase diagram. Phase separation at 265°C occurred in Region II of the phase diagram, whereas phase separation at 290 and 300°C occurred in the shallow and deep regimes, respectively, of Region III of the phase diagram. Phase separation in Region II is powered by the high molecular mobility of the PC segments. On the other hand, both of the molecular mobilities of LCP and PC contribute to the phase separation in Region III. For the 10 wt % LCP/PC blends, the coarsening process during the late stage of spinodal decomposition can be attributed to the diffusion-coalescence mechanism. For the 20 wt % LCP/PC blends, three coarsening mechanisms can occur at the same time. These include the vanishing of PC-rich domains through the evaporation-condensation mechanism, the combining of LCP-rich domains through diffusion-coalescence, and the breakup of LCP-rich network-like structure driven by capillary pressure gradients. The reorientation of the LCP segments ordering showed a time lag behind the concentration ordering.

APPENDIX A: FTIR MICROSCOPY

FTIR microscopy was used to investigate the concentration profiles of the phase-separated LCP/PC blends. Samples for FTIR microscopy experiments were prepared in the same method as samples for optical microscopy, except that the samples were sandwiched between two sheets of fiber-glass reinforced Teflon before loading into the sample cell. With this arrangement, the phase-separated samples could be removed from the cell for FTIR microscopy experiments without damage. All the samples for FTIR microscopy experiments were annealed at 300°C for 20 minutes. Therefore, the phase-separated

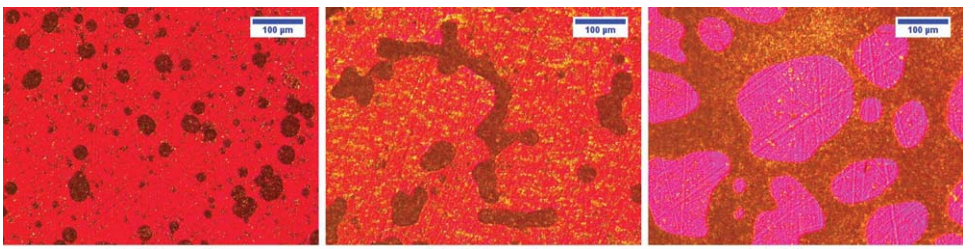

Figure A1 Morphological structures of (a) 10 wt %, (b) 20 wt %, and (c) 50 wt % LCP/PC blends under the polarized light microscope. Scale bars on the images represent 100 μm. [Color figure can be viewed in the online issue, which is available at www.interscience.wiley.com.]

structures in these samples were obtained from the very late stage of phase separation.

Infrared spectra of the samples were recorded by using an IR microscope (Bruker Optics Hyperion 2000, Billerica, MA) in conjunction with a FTIR spectrometer (Tensor 27 with liquid-nitrogen MCT detector). Transmitted spectra at the selected positions of the sample were recorded between 4000 and 400 cm^{-1}, with 30 scans at a resolution of 4 cm^{-1}. The knife edge apertures were set to 7 μm by 7 μm, to allow sufficient light to pass through the sample while maintaining as high spatial resolution as possible.

Before the FTIR microscopy experiments, samples were examined under the PLM. Figure A1 shows the pictures of phase-separated structures observed with the PLM for (a) 10 wt %, (b) 20 wt %, and (c) 50 wt % LCP/PC blends. These images are similar to those shown in Figures 5–7. In these images violet color is consider as the PC-rich phase, whereas brownish-yellow is consider as LCP-rich phase.

Figure A2 shows the phase-separated structures obtained by optical microscopy (top row) and FTIR transmission intensity at 1770 cm^{-1} wave-number at various positions along the red line drawn on the samples (bottom row) for (a) 10 wt %, (b) 20 wt % and (c) 50 wt % LCP/PC blends. Previous studies showed that the characteristic carbonyl stretching bands for PC and LCP were located at $\sim$ 1770 and $\sim$ 1730 cm^{-1}, respectively.[27] In this article, transmission intensity at wave-number 1770 cm^{-1} was selected to represent the PC concentration. Thus, positions with high content of PC show high transmission intensity, whereas positions with low transmission intensity are rich in LCP. For all the cases shown in Figure A2, regions with high transmission intensity are located in the light gray sections that appear in the optical microscopy images. On the other hand, positions with low transmission intensity appear in black in the optical microscopy images. Comparison with images in Figure A1, it

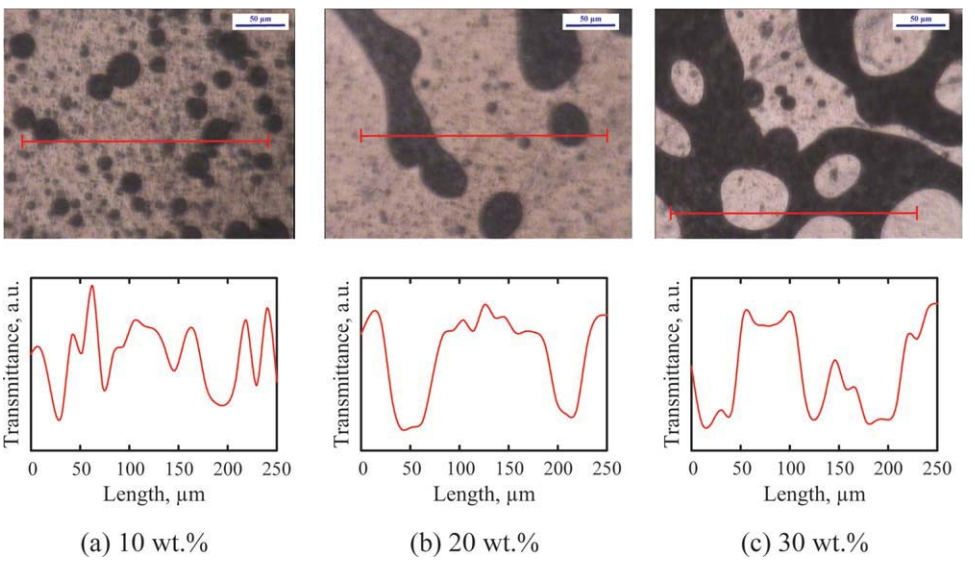

Figure A2 Phase-separated structures (top row) and transmission intensity at wave-number of 1770 cm^{-1} at various positions (bottom row) for (a) 10 wt %, (b) 20 wt %, and (c) 50 wt % LCP/PC blends. The regions of transmission intensity measurements are drawn as red lines on the morphological images. Scale bars on the images represent 50 μm. [Color figure can be viewed in the online issue, which is available at www.interscience.wiley.com.]

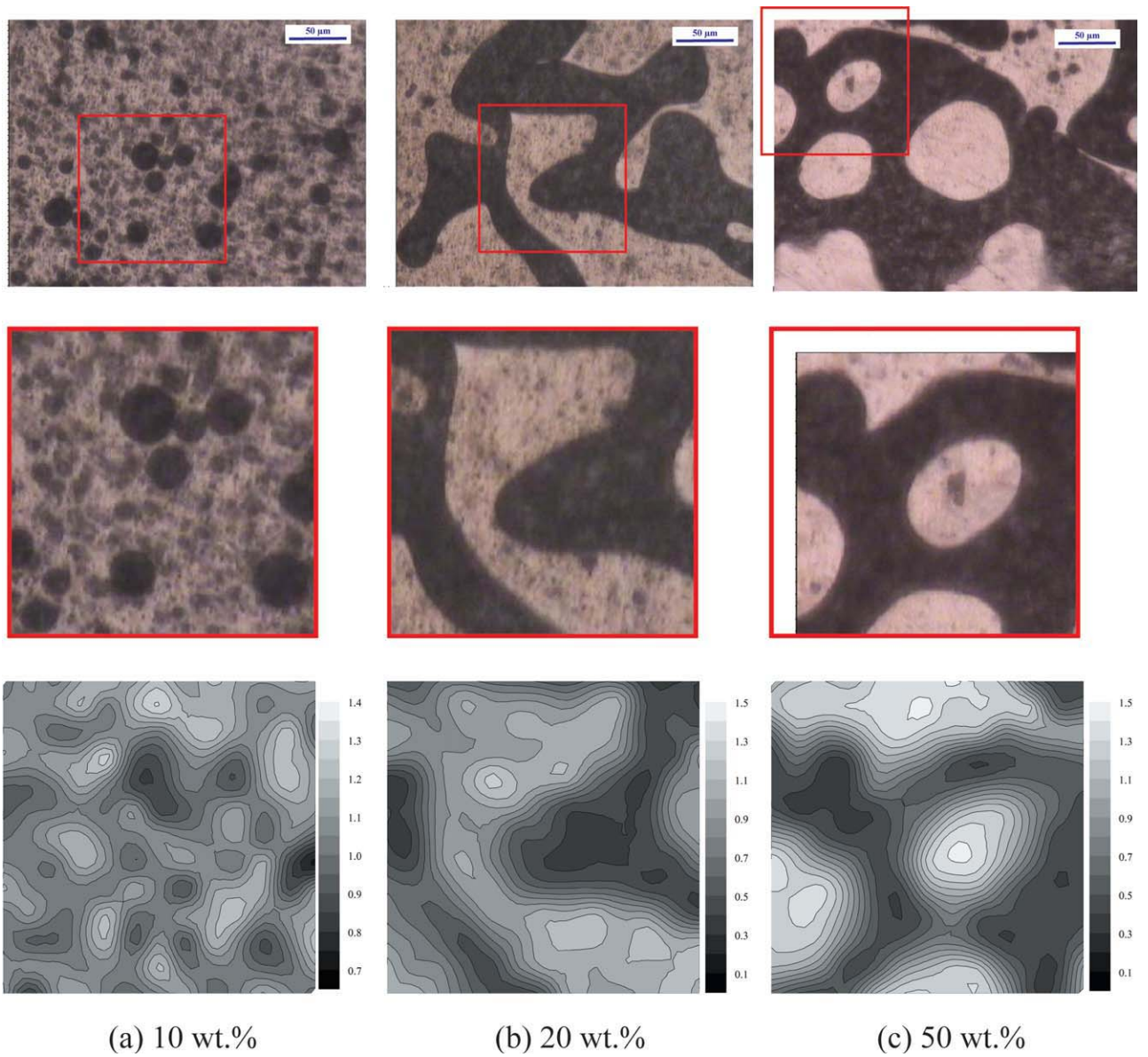

Figure A3 Phase-separated structures (top row) and contours of FTIR transmission intensity at wave-number of 1770 cm^{-1} (bottom row) for (a) 10 wt %, (b) 20 wt %, and (c) 50 wt % LCP/PC blends. Regions for two-dimensional mapping are marked as red boxes on the optical microscope images and the enlarged images are shown in the middle row. The size of the scanning region is 128 μm × 128 μm for all the cases. [Color figure can be viewed in the online issue, which is available at www.interscience.wiley.com.]

shows that the light gray color corresponds to the violet color under the PLM and the black corresponds to the brownish-yellow color. This suggests that the PC-rich phase and the LCP-rich phase appear as violet and brownish-yellow under the PLM, respectively.

Two dimensional mapping of the phase-separated structures was also performed with a similar approach as for one-dimensional scanning. Figure A3 presents the phase-separated structures (top row) and the contours of the FTIR transmission intensity at 1770 cm^{-1} wave-number, obtained from selected regions in the samples (bottom row) for (a) 10 wt %, (b) 20 wt % and (c) 50 wt % LCP/PC blends. Regions for two-dimensional scanning are marked as red boxes on the morphological images (top row). Enlarged images of these regions are shown in the middle row of the figure. The areas of the scanning zones are 128 μm × 128 μm. The contour plots of the FTIR transmission intensity at 1770 cm^{-1} wave-number are shown, using gray scale, in Figure A3. The light and dark gray colors represent high and low transmission intensity, respectively. In other words, regions with high content of PC are displayed as light gray, whereas areas with high concentration of LCP are shown as dark gray. In

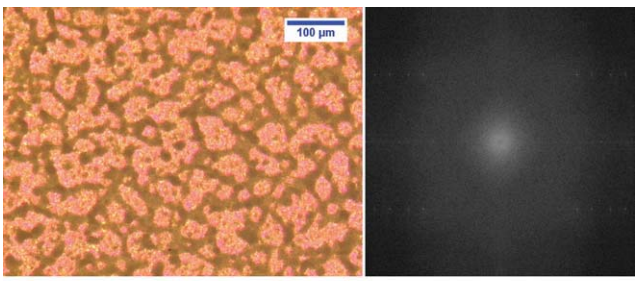

(a) 0 min.

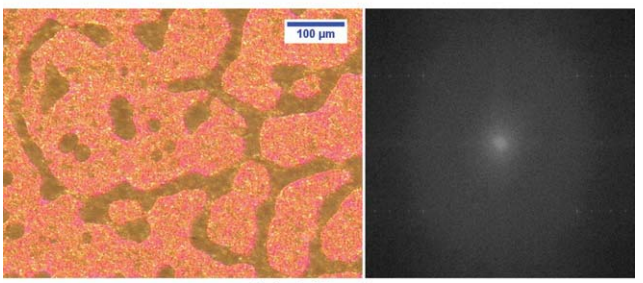

(b) 4.92 min.

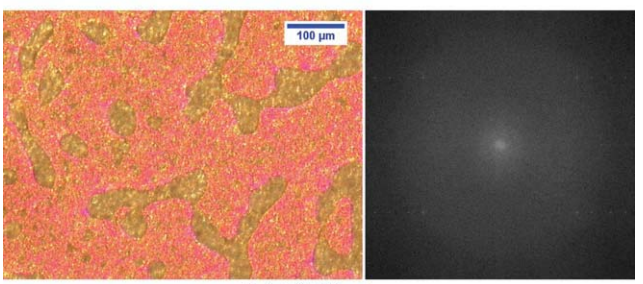

(c) 18.18 min.

Figure B1 Phase-separated structure in real space (left column) and the corresponding power spectrum of FFT in wave-number space (right column) of 20 wt % LCP/PC blends at different annealing times at 300°C. [Color figure can be viewed in the online issue, which is available at www.interscience.wiley.com.]

comparison with the optical microscope images, the contour plots of the FTIR transmission intensity agree well with the observed phase-separation in the blends. This further supports the observation that the PC-rich phase appears as violet under the PLM, whereas the LCP-rich phase is displayed as brownish-yellow.

APPENDIX B: DIGITAL IMAGE ANALYSIS OF PHASE-SEPARATED STRUCTURES OF LCP/PC BLENDS

Digital image analysis (DIA) was employed to characterize the growth of the phase-separated structures of LCP/PC blends in the wave-number space (k). DIA is a useful tool to extract wide variety of physical information from an image that is obtained under an optical microscope.[43] Using DIA, an image of structure of a polymer system in real space can be converted to a power spectrum image in wave-number space by two-dimensional Fourier transformation (2DFT). The power spectrum image in the wave-number space can then be related to an image obtained by a light scattering experiment, such as small-angle light scattering, which has frequently been used for studying phase separation in polymer systems. Therefore, structural parameters in light scattering theories can also be applied to physical information obtained from 2DFT images. It is known that a 2DFT image in wave number space corresponds to an image obtained by small-angle light scattering, when a phase contrast microscope is used.[43] As a result, the power spectrum image from 2DFT operation of an original image from phase contrast microscopy is equivalent to the scattering intensity. Moreover, in the case of polarizing microscopy, a 2DFT image in wave number space is not equivalent to the scattering intensity, but the information obtained is similar.[43]

The power spectra of the phase-separated structures of the LCP/PC blends in this study were obtained by FFT of the original image in real space by using the software ImageJ.[44] The radial intensity distribution of the power spectrum was obtained by taking the average of each radial distance from the origin of the FFT image to further study the phase separation characteristic of this blend. Figure B1 demonstrates the phase separated structures of 20 wt % LCP/PC blends, observed during annealing at 300°C under a PLM (left column) at various phase separation times, and the corresponding power spectra obtained from FFT (right column). These power spectrum images are similar to those commonly observed from light scattering experiments. The ring

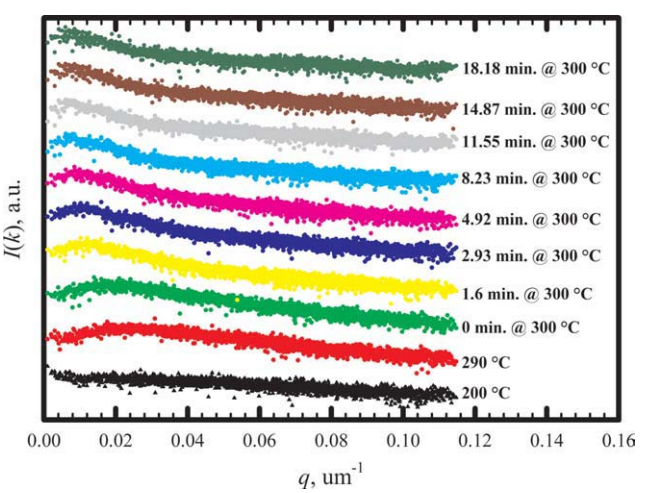

Figure B2 Temporal change of the radial intensity distribution in wave number space, $I(k)$, of the phase-separated structures in the 20 wt % LCP/PC blends. [Color figure can be viewed in the online issue, which is available at www.interscience.wiley.com.]

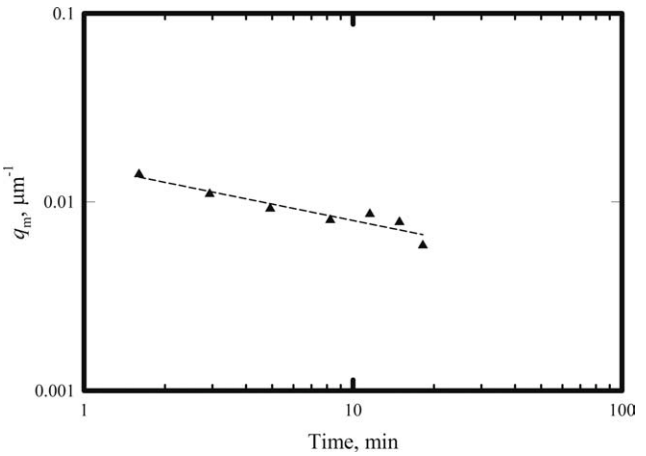

Figure B3 Double-logarithmic plot of temporal development of q_m against phase separation times of 20 wt % LCP/PC blends at 300°C.

at the center region of the power spectrum becomes smaller and moves towards the origin with time. This is similar to the so-called spinodal ring, which is a characteristic of the spinodal decomposition. Thus, these results support the conclusion that the phase separation process occurring in this blend underwent spinodal decomposition. Similar results were obtained for the 50 wt % LCP/PC blend experiments.

Analysis of temporal change of phase-separated structures is necessary for studying the dynamics of phase separation. Figure B2 shows the temporal change of the radial intensity distribution in wave number space, $I(k)$, of the phase-separated structures in the 20 wt % LCP/PC blends. It should be mentioned that these distributions were vertically shifted for the purpose of better visual presentation. These intensity distribution profiles are also similar to the temporal development of the structure factors resulting from spinodal decomposition by using light scattering experiments. The shape of $I(k)$ can then be compared with the theory of spinodal decomposition. The peak position of $I(k)$ corresponds to the characteristic wavelength of the concentration fluctuation, whereas the peak width is connected to its distribution. Figure B2 indicates that the phase separation occurring in these blends can be divided into two stages. In the first stage, phase separation of the blends occurs in the second heating ramp of the heating profile (see the experimental section in the main text), that is, before reaching the temperature for isothermal phase separation. In this stage, peaks of $I(k)$ are not obvious and the position of the peak with maximum intensity, q_m, remains relatively unchanged. This seems to be the so-called early stage of the spinodal decomposition. However, in the second stage, q_m shifts toward a lower value of the wave-number with increasing time. The decrease in q_m with time implies the growth of the phase-separated domains. This stage corresponds to the late stage of the spinodal decomposition.

Figure B3 shows a double-logarithmic plot of the temporal development of q_m during the phase separation of 20 wt % LCP/PC blends, at different isothermal annealing times. This curve supports the decreasing trend of the radial intensity distribution peaks to lower wave-numbers. The slope of this curve is −0.29, corresponding to the growth of the phase-separated domains in the late stage of the spinodal decomposition. This value is somewhat smaller than the conventional theoretical value of −1/3.

References

1. Su, Y.; Chen, C.; Li, Y.; Li, J. J Macromol Sci Pure Appl Chem 2007, 44, 99.
2. Chen, G.; Lin, Y.; Wang, X. J Appl Polym Sci 2007, 105, 2000.
3. Zhang, X.; Wang, Z.; Han, C. C. Macromolecules 2006, 39, 7441.
4. Pang, Y.; Dong, X.; Zhao, Y.; Han, C. C.; Wang, D. Polymer 2007, 48, 6395.
5. Tanaka, T.; Tsuchiya, T.; Takahashi, H.; Taniguchi, M.; Ohara, H.; Lloyd, D. R. J Chem Eng Jpn 2006, 39, 144.
6. Yang, F.; Qu, X.; Cui, W.; Bei, J.; Yu, F.; Lu, S.; Wang, S. Biomaterials 2006, 27, 4923.
7. Gong, Y.; Ma, Z.; Gao, C.; Wang, W.; Shen, J. J Appl Polym Sci 2006, 101, 3336.
8. Araki, T.; Tran-Cong, Q.; Shibayama, M., Eds. Structure and Properties of Multiphase Polymeric Materials; Marcel Dekker: New York, 1998
9. Sperling, L. H. Introduction to Physical Polymer Science, 4th ed.; Wiley: Hoboken, 2006.
10. Zhao, J.; Lu, X.; Chen, Y.; Chow, L. K.; Chen, G.; Zhao, W.; Samper, V. J Mater Process Technol 2005, 168, 308.
11. Zhuang, P.; Kyu, T.; White, J. L. Polym Eng Sci 1988, 28, 1095.
12. Nobile, M. R.; Amendola, E.; Nicolais, L.; Acierno, D.; Carfagna, C. Polym Eng Sci 1989, 29, 244.
13. Kyu, T.; Zhuang, P. Polym Commun 1988, 29, 99.
14. Nagaya, T.; Orihara, H.; Ishibashi, Y. J Phys Soc Jpn 1989, 58, 3600.
15. Siegmann, A.; Dagan, A.; Kenig, S. Polymer 1985, 26, 1325.
16. Kiss, G. Polym Eng Sci 1987, 27, 410.
17. Isayev, A. I.; Modic, M. Polym Compos 1987, 8, 158.
18. Weiss, R. A.; Huh, W.; Nicolais, L. Polym Eng Sci 1987, 27, 684.
19. Ko, C. U.; Wilkes, G. L.; Wong, C. P. J Appl Polym Sci 1989, 37, 3063.
20. Zaldua, A.; Munoz, M. E.; Pena, J. J.; Santamaria, A. Polym Adv Technol 1994, 5, 423.
21. Engberg, K.; Strömberg, O.; Martinsson, J.; Gedde, U. W. Polym Eng Sci 1994, 34, 1336.
22. Turek, D. E.; Simon, G. P.; Tiu, C. Polym Eng Sci 1995, 35, 52.
23. Ruggiero, V.; Acierno, D. Adv Polym Tech 2007, 26, 109.
24. Cohen-Addad, S.; Stein, R. S.; Esnault, P. Polymer 1991, 32, 2319.
25. Zheng, J. Q.; Kyu, T. Polym Eng Sci 1992, 32, 1004.
26. Nakai, A.; Shiwaku, T.; Wang, W.; Hasegawa, H.; Hashimoto, T. Macromolecules 1996, 29, 5990.
27. Lee, K.-W. D.; Chan, P. K.; Kamal, M. R. J Appl Polym Sci 2009, 111, 396.

28. Kramer, E. J.; Green, P.; Palmstrøm, C. J. Polymer 1984, 25, 473.
29. Chan, P. K. Mater Res Soc Symp Proc 2002, 710, 37.
30. Tanaka, H.; Yokokawa, T.; Abe, H.; Hayashi, T.; Nishi, T. Phys Rev Lett 1990, 65, 3136.
31. Kyu, T.; Mustafa, M.; Yang, J.-C.; Kim, J. Y.; Palffy-Muhoray, P. Stud Polym Sci 1992, 11, 245.
32. Copetti, M. I. M.; Elliott, C. M. Mater Sci Technol 1990, 6, 273.
33. Chakrabarti, A. Phys Rev B 1992, 45, 9620.
34. Chan, P. K.; Rey, A. D. Macromol Theory Simul 1995, 4, 873.
35. Blizard, K. G.; Baird, D. G. Polym Eng Sci 1987, 27, 653.
36. Choy, C. L.; Lau, K. W. E.; Wong, Y. W.; Ma, H. M.; Yee, A. F. Polym Eng Sci 1996, 36, 827.
37. Binder, K.; Stauffer, D. Phys Rev Lett 1974, 33, 1006.
38. Lifshitz, I. M.; Slyozov, V. V. J Phys Chem Solids 1961, 19, 35.
39. Siggia, E. D. Phys Rev A 1979, 20, 595.
40. Wang, X.-J.; Zhou, Q.-F. Liquid Crystalline Polymers; World Scientific: New Jersey, 2004.
41. Kim, D.; Kyu, T.; Hashimoto, T. J. Polym Sci B: Polym Phys 2006, 44, 3621.
42. Ahn, W.; Ha, K.; Park, L. S. Mol Cryst Liq Cryst 2006, 458, 191.
43. Konno, M.; Nishikori, Y.; Saito, S. J Chem Eng Japn 1993, 26, 33.
44. Rasband, W. S. ImageJ 1997–2007; U.S. National Institutes of Health: Bethesda, MD. Available at: http://rsb.info.nih.gov/ij/. Accessed April 23, 2009.